

# Intelligent Demand Response for Industrial Energy Management Considering Thermostatically Controlled Loads and EVs

Jidong Wang, *Member, IEEE*, Yingchen Shi and Yue Zhou, *Member, IEEE*

**Abstract**—In this paper, an intelligent energy management framework with demand response capability was proposed for industrial facilities. The framework consists of multiple components, including industrial processes modeled by the state task network (STN) method, thermostatically controlled loads (TCLs) like the heating, ventilation and air conditioning (HVAC) system with chilled water storage (CWS), renewable generation like photovoltaic (PV) arrays and electric vehicles (EVs). These components were firstly modeled and the operation of them is then optimized in time-of-use (TOU) pricing schemes. Factors that affect several components at the same time, e.g. the number of workers, are considered. The optimization is formulated as a mixed integer linear programming (MILP) problem. A general tire manufacturing facility was investigated as the case study. Simulation results show that the proposed intelligent industrial energy management (IEM) with DR is able to effectively utilize the flexibility contained in all parts of the facility and reduce the electricity costs as well as the peak demand of the facility, while satisfying all the operating constraints.

**Index Terms**—Industrial demand response, industrial energy management, state task network, thermostatically controlled loads, chilled water storage, electric vehicles.

## I. INTRODUCTION

THE continuous development of smart grid provides technical support for the full play of demand response resources. Demand response (DR), in which customers are able to actively adjust their pattern of power consumption, is considered as one of the most promising solutions to release the stresses of power systems [1]. So far, there have been a large number of studies about applying smart grid technologies to residential and commercial consumers [2]-[4], but relatively fewer studies have been made in industrial sectors. This is mainly because the potential of smart grids for industrial sectors has not been fully tapped, especially in the background

This work was supported in part by the National Natural Science Foundation of China (51477111), in part by National Key Research and Development Program of China (2016YFB0901102) and in part by the Flexis (Flexible Integrated Energy Systems) project. Flexis is part-funded by the European Regional Development Fund (ERDF) through the Welsh Government. Paper no. TII-18-2053. (*Corresponding author: Yue Zhou.*)

Jidong Wang and Yingchen Shi are with the Key Laboratory of Smart Grid of Ministry of Education, Tianjin University, Tianjin 300072, China (e-mail: jidongwang@tju.edu.cn; yeshi@tju.edu.cn). Yue Zhou is with the School of Engineering, Cardiff University, Cardiff CF24 3AA, United Kingdom (e-mail: ZhouY68@cardiff.ac.uk)

of smart grid with many new technologies developed [5]. Also as pointed out in [5], compared with other customer sectors, industrial facilities are less involved in the definition, standardization, and research work related to smart grids. On the other hand, industrial facilities are energy-intensive users and nearly 70% of electricity is consumed by industry in China by 2017 [6]. As the world's electricity consumption continues to grow, traditional power systems are facing limitations such as the insufficiency of transformer capacity. Therefore, implementing DR in industrial sectors are of great potential and significance. For industrial facilities, energy consumption and costs are able to be reduced with the energy efficiency increased. For power systems, the safety and reliability are able to be strengthened.

However, in some aspects it is more complex to carry out DR for industrial facilities than residential and commercial ones, because many factors have to be considered in the electricity analysis of industrial processes, such as the continuity between industrial processes and the flow between materials. [7] provided a method based on state task network (STN) to carry out DR in the industrial user side, which suits actual industrial facilities well. [8] proposed a mathematical structure to realize optimal load control for industrial facilities. An oil refinery was considered as an example to illustrate the unique characteristics of industrial processes. [9] made further improvements in four aspects based on the work of [8], taking the smart grid factors into account. An algorithm for industrial load control is described in [10], but with some important features of industrial facilities ignored. In [11], an industrial DR scheme was proposed for industrial processes based on STN, taking full use of energy generation/storage systems. The proposed method was verified in a case of oxygen generation facilities.

In addition to the power consumption of industrial processes, industrial facilities also involve temperature control of the plants during production processes. Therefore, thermostatically controlled loads (TCLs) need to be considered in industrial energy management. [12] developed a new air-conditioning system, which contains a chilled water storage (CWS) system with temperature and humidity control and reduces power consumption compared with traditional air-conditioning systems. [13] proposed a novel hybrid algorithm based on Ant-Based Radial Basis Function Network to deal with the ice storage air-conditioning system and the optimization results demonstrate that reasonable solutions can improve the

dispatching chillers energy efficiency greatly, thus reducing the buildings electricity expenses. Considering the unique characteristics of industrial processes, the optimal chiller scheduling for a CWS in an automotive manufacturing plant was studied by [14] in order to minimize the electricity costs of industrial facilities.

Although there have been a number of existing studies as described above, they did not study the DR and energy management strategies for modern industrial facilities that are equipped with TCLs and low-carbon technologies (i.e. renewable generation and electric vehicles (EVs) at the same time. Energy vehicles, as an important means to facilitate low-carbon transportation, are encouraged in many countries across the world, and are expected to develop very fast in the near future [15]. Given the widespread use of EVs by workers in the future, new smart grid technologies such as vehicle-to-grid (V2G) should also be taken into account. [16] described an efficient and robust mixed integer linear programming (MILP) model for the coordination of plug-in EVs charging in electricity distribution systems. Considering the V2G technology of EVs, the coordinated control of energy storage and EVs in electricity distribution systems was devised to determine the optimal charging time for energy storage devices and EVs in [17]. In [18], an intelligent energy management system was proposed for industrial facilities with various PV generation capacity, but it fails to consider the important role that EVs play in power systems.

In this paper, an intelligent industrial energy management (IIEM) framework integrated with DR is proposed to optimally manage industrial processes as well as associated equipment including TCLs, EVs and photovoltaic (PV) panels. Mathematically, the optimal management problem is modeled as a MILP problem. The objective function minimizes the energy cost of the industrial facilities given time-of-use electricity prices, and the linear constraints are modeled to guarantee the normal operation of industrial process and take full advantage of the flexibility contained in TCLs and EVs. The performance of the proposed method is evaluated using the example of a tire manufacturing facility, and the simulation results verify the effectiveness and advantage of the proposed method.

The contributions of this paper are summarized as follows.

(i) The proposed IIEM optimally schedules the operation of industrial processes as well as TCLs and charging/discharging of EVs in an industrial facility with PV generation. This work has not been presented in existing literature, and is able to optimize the operation of industrial facilities in the background of smart grid.

(ii) In the formulation of the proposed IIEM, the effects of the number of workers on the operation of industrial processes, the number of EVs and the temperature of industrial workshops (which is related to TCLs) are all considered and formulated in the corresponding constraints, so that the optimization results can better reflect the reality. In the existing literature, the impact of the number of workers has not been considered that comprehensively.

(iii) In the formulation of proposed IIEM, the thermal loads

are modelled by composition in details, which can result in more accurate thermal load estimation and hence more accurate optimization results. Most existing studies failed to conduct such detailed analysis in the optimization of industrial processes.

## II. IIEM FRAMEWORK AND PROBLEM FORMULATION

### A. IIEM Framework with DR

The framework of IIEM with DR is shown in Fig. 1.

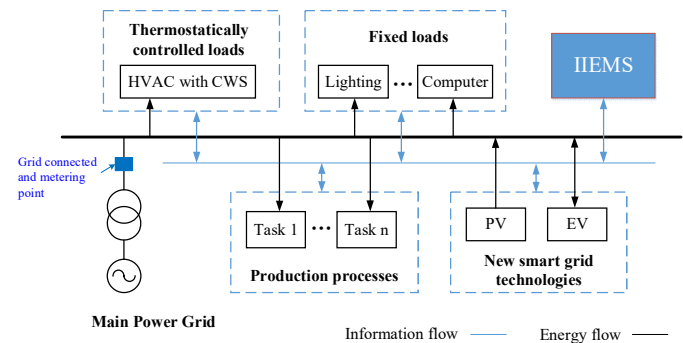


Fig. 1. The framework for intelligent industrial energy management.

The intelligent industrial energy management system (IIEMS) shown in Fig. 1 receives the electricity price signals from the power utility and schedules the electricity demand of the industrial facility using the best DR schemes with the embedded algorithms. The demand consists of industrial processes with various tasks, low-carbon devices such as PV and EVs, thermostatically controlled loads such as the heating, ventilation and air conditioning (HVAC) systems with CWS system, and fixed loads such as lighting and computers. Both the PV generation and discharging of EVs are able to serve as power sources for all or part of the industrial facility. The industrial facility can also sell excess energy to the utility besides purchasing power from the main grid.

Whether the scheduling of EVs and industrial processes are coupled with each other depends on the electrical configuration, metering scheme used, how the electricity is sold to the bulk power grid, and the relationship between the prices for buying and selling electricity from/to the bulk power grid. The electrical configuration and metering scheme considered in this paper are illustrated in Fig. 1, in which the whole industrial facility has only one grid-connected and metering point at the transformer. As a result, the local PV generation has to be consumed on-site first to supply local loads in the industrial facility, with just excess generation exported to the bulk power grid. In other words, in this case, it is not possible to export all the local PV generation to the grid and at the same time satisfy all the local loads with the electricity imported from the grid. This electrical configuration and metering scheme are widely used in practice [11], [18]. Furthermore, in this paper, it is assumed that the electricity sold to the grid is directly compensated at the feed-in tariff rates. However, if other mechanisms are used, such as the “net metering” mechanism in which the excess electricity fed into the grid is recorded and deducted from the usage in the future, the strategy for

scheduling EVs and industrial processes may be different.

In this situation, whether the scheduling of EVs and industrial processes are coupled depends on the relationship between the buying and selling prices. If the selling price at any time is equal to the buying price at any time throughout the day, the scheduling of EVs and industrial processes are decoupled, because in these cases there is no difference between using local PV generation and using electricity imported from the bulk power grid for both EVs and industrial processes. In all the other cases, the situation is very complex. For example, if the selling price is constant and lower than the buying price at any time, the EVs and industrial processes should be scheduled collectively to utilize the excess local PV generation to the maximum extent and at the same time import electricity from the grid as cheap as possible throughout the day. Similarly, if the selling price is constant but higher than the buying price at any time, the EVs and industrial processes should be jointly scheduled as well to make local PV generation exported to the grid to the maximum extent and at the same time import electricity from the grid as cheap as possible throughout the day. However, the price structure may be very complex. For example, throughout the day, at some periods, buying prices may be higher than selling prices, but at the other periods, the buying prices may be lower than selling prices. Furthermore, it is possible that the selling price at a period is higher than the buying price at the same period, but being lower than the buying prices at other periods. In these cases, considering the load shifting capability of EVs and industrial processes, their scheduling are very likely to be coupled with each other, but there is no known general theoretical tools that can make this judgement (i.e. coupled or not coupled) a priori to the best of our knowledge. In this paper, the buying and selling prices change over the day and their magnitudes vary, so the EVs and industry processes can be shifted to optimize the net income/cost of the whole industrial facility.

Considering the above fact, in the IEM proposed in this paper, the scheduling of EVs and industrial processes are conducted collectively in an optimization problem rather than individually. This is because to optimize them collectively will obtain no worse results than do it individually, and can always get the optimal results no matter what buying and selling prices are adopted.

Besides, the operation of EVs and industrial processes is also indirectly related to each other through the number of workers of a shift. The number of workers of a shift directly decides the number of EVs available during the shift, and also constrains what and how many industrial processes are able to operate during a shift. This means that, when making the schedules, the constraints of EVs and industrial processes at a time slot are correlated with each other. In this paper, this correlation does not justify that the scheduling of EVs and industrial processes needs to be conducted at the same time, because it is assumed the number of each shift is constant. However, if the number of workers are considered as a decision variable in future studies, this correlation will further increase the coupling between the scheduling of EVs and industrial processes in an industrial facility.

## B. Industrial Process Modeling

The State Task Network (STN) framework was first proposed in [19] to handle multiproduct batch chemical plants, and further used in [7] and [11] to conduct demand response studies for steel manufacturing and oxygen generation facilities. The STN framework describes an industrial facility as networked task nodes and state nodes, representing industrial processes and materials involved respectively. The STN framework formulates industrial facilities in a general way, so has the potential to be applied to model many other industrial facilities. In this paper, the STN framework is used to describe industrial processes.

The scheduling problem is represented by discrete time, where the scheduling horizon is divided into equal time slots expressed by  $\Delta t$ . It is assumed that parameters are constant in each time intervals, so that each moment  $t$  can represent each time interval  $(t, t+1)$ .

### 1) Task Nodes

Industrial processes in an industrial facility can be categorized as schedulable and nonschedulable ones. Schedulable industrial processes can operate at multiple statuses, with different power consumption levels, material consumption rates, production rates, etc. These statuses at which an industrial process can operate, are called ‘operation states’ of the industrial process.

For example, in the tire manufacturing facility that will be studied in the case study section of this paper (Section III), the ‘Moulding and Curing (M&C)’ process, which takes tread, bead and carcass components as the inputs and produces tires as the output, can be seen as a schedulable industrial process. The M&C process can operate at three different operation states, consuming 450kW, 600kW and 750kW electric power and producing 150, 200 and 250 tires per hour respectively. Details can be found in Section III.

In addition, how long an operation state should last, depends on the required quantity of its products and its production capability. For example, if 1000 tires are required to be produced within a day, then the M&C process with the production rate being 250 tires per hour needs to operate 4 hours. How to allocate these 4 hours within a day depends on the production of the input materials, and also the consideration to minimize the electricity bill with electricity prices, PV generation, etc. taken into account.

Described in the STN model, for each schedulable task (i.e. schedulable process)  $i$ , parameters of operation state  $k$  is associated with electricity demand  $p_{i,k}$ , number of workers  $w_{i,k}$ , equipment heat dissipation  $q_{i,k}$ , material consumption rate  $a_{i,j,k}$  and productivity rate  $b_{i,j,k}$  of state  $j$ . Besides, a binary variable  $x_{i,k,t}$  is defined to indicate whether the task  $i$  operates at point  $k$  at time slot  $t$ .

For a specific task  $i$ , the electricity demand  $P_{i,t}$ , number of workers  $W_{i,t}$ , equipment heat dissipation  $Q_{i,t}$  of task  $i$  at time slot  $t$  can be described as

$$P_{i,t} = \sum_{k=1}^m x_{i,k,t} p_{i,k} \quad (1)$$

$$W_{i,t} = \sum_{k=1}^m x_{i,k,t} w_{i,k} \quad (2)$$

$$Q_{i,t} = \sum_{k=1}^m x_{i,k,t} q_{i,k} \quad (3)$$

where  $m$  represents the amount of operation states in task  $i$ .

The material quantity of state  $j$  consumed and produced by task  $i$  at time slot  $t$  are described as

$$c_{i,j,t} = \sum_{k=1}^m x_{i,k,t} a_{i,j,k} \quad (4)$$

$$g_{i,j,t} = \sum_{k=1}^m x_{i,k,t} b_{i,j,k} \quad (5)$$

where  $c_{i,j,t}$  and  $g_{i,j,t}$  are the material quantity of state  $j$  consumed and produced by task  $i$ .

At each time slot  $t$ , schedulable task (ST)  $i$  only operates on one operation state at any time slot, as constrained by

$$0 \leq \sum_{k=1}^m x_{i,k,t} \leq 1 \quad (6)$$

which ensures that only one  $x_{i,k,t}$  of task  $i$  is equal to 1 and the others are forced to be 0.

However, for nonschedulable tasks (NSTs), the state variables cannot be changed, i.e.,

$$x_{i,k,t} = x_{i,k,t}^{set} \quad (7)$$

where  $x_{i,k,t}^{set}$  represents the fixed operation state set by the industrial facilities at time slot  $t$ .

In addition, the total number of workers needed for all the tasks, plus the ones working in the office, should not exceed the total number of workers of each shift:

$$\sum_{i=1}^I W_{i,t} + W_n^{fix} \leq W_n \quad (8)$$

where  $I$  is the amount of industrial tasks;  $W_{i,t}$  is the number of workers needed for industrial task  $i$  at the time slot  $t$ ;  $W_n^{fix}$  represents the number of workers working in the office at the shift  $n$ , which is assumed to be constant in each shift in this paper;  $W_n$  represents the total number of workers of the shift  $n$ , which is also assumed to be constant for each shift in this paper.

### 2) State Nodes

The state nodes, including raw materials, intermediates and final products, are related to the task nodes that produce and consume materials stored in the corresponding state nodes.

The material balance constraint of each state is expressed as

$$S_{j,t+1} = S_{j,t} + \left( \sum_{i \in G_j} g_{i,j,t} - \sum_{i \in C_j} c_{i,j,t} \right) \Delta t \quad (9)$$

where  $S_{j,t}$  is the storage of state  $j$  at each time slot  $t$ ;  $G_j$  and  $C_j$  represent the set of tasks that produce and consume at state  $j$  respectively.

For the normal operation of industrial processes, the storage  $S_{j,t}$  of each state  $j$  at any time slot  $t$  must satisfy the storage constraints, i.e.,

$$S_j^{\min} \leq S_{j,t} \leq S_j^{\max} \quad (10)$$

where  $S_j^{\min}$  and  $S_j^{\max}$  represent the and upper limits respectively.

Generally, industry facilities have a daily production requirement for the corresponding state node, i.e.,

$$S_{j,T} - S_{j,1} \geq S_j^{set}, \quad j \in \mathbf{J} \quad (11)$$

where  $T$  is the end of the time horizon, so  $S_{j,T}$  and  $S_{j,1}$  represent the final and initial storage of state  $j$  respectively.

$\mathbf{J}$  is the set of final products.  $S_j^{set}$  is the minimum amount of final product that is needed.

For those nonstorable state nodes, i.e., the material must be sent to the next task as soon as it is produced. This constraint is formulated as

$$S_{j,t} = 0 \quad (12)$$

### C. Thermostatically controlled load Modeling

#### 1) Thermal Dynamic Balance Equation of an Industrial Plant

The TCLs in industrial plants are built to ensure product quality, the safe operation of production equipment and necessary environmental conditions. According to the design specification for HVAC, the temperature constraint in the plant at time slot  $t$  can be expressed as

$$\theta_{in,t}^{down} \leq \theta_{in,t} \leq \theta_{in,t}^{up} \quad (13)$$

where  $\theta_{in,t}$  is the temperature in the plant;  $\theta_{in,t}^{down}$  and  $\theta_{in,t}^{up}$  are the lower and upper limits of the temperature of the industrial plant at each time slot.

Generally, the cooling power  $Q_{c,t}$  equals to the sum of total heat gain of the industrial plant, the heat storage of building envelope and fresh air heat at time slot  $t$ . The total heat gain  $Q_{tot}$  mainly includes the heat transfer from building envelope  $Q_{trs}$ , solar radiation  $Q_{sol}$ , electrical equipment  $Q_{eq}$  and workers  $Q_w$ . To simplify, the total heat gain  $Q_{tot}$  at each time slot [20] can be formulated as

$$Q_{tot,t} = B(\theta_{out,t} - \theta_{in,t}) + Q_{sol,t} + Q_{eq,t} + Q_{w,t} \quad (14)$$

where  $B$  is the sum of the heat transfer coefficient and the fresh air specific heat coefficient of the industrial buildings;  $\theta_{out,t}$  is the ambient temperature at time slot  $t$ . Note that the heat transfer through both air convection and building envelope has been considered in the coefficient  $B$ , which is calculated by

$$B = 0.28G + KF \quad (15)$$

where  $G$  is the fresh air volume;  $K$  and  $F$  represent the heat transfer coefficient and the area of building envelope respectively. Equation (15) and the methods to decide the values of the parameters in (15) can refer to the Chinese standard [21].

In particular, the total electrical equipment heat dissipation  $Q_{eq,t}$  and workers heat dissipation  $Q_{w,t}$  at time slot  $t$  can be formulated as

$$Q_{eq,t} = \sum_{i=1}^I Q_{i,t} + q_{eq}^{fix} \quad (16)$$

$$Q_{w,t} = q_w W_n \quad (17)$$

where  $q_{eq}^{fix}$  is the fixed heat dissipation of electrical equipment such as lighting, computers and printers;  $q_w$  is the sensible heat per person.

According to the conservation law of energy, the thermal dynamic equilibrium equation in the plant can be derived as

$$C_a V \rho_a d\theta_{in} = (Q_c - Q_{tot}) dt \quad (18)$$

where  $C_a$  is the air constant pressure mass ratio heat capacity;  $V$  is the volume of the industrial plant;  $\rho_a$  is the air density.

Formula (18) is discretized to derive the thermal dynamic equilibrium equation in discrete form, i.e.,

$$\theta_{in,t+1} = \theta_{in,t} e^{-R\Delta t} + (1 - e^{-R\Delta t}) \left( \frac{Q_{sol,t} + Q_{w,t} + Q_{eq,t} - Q_{c,t}}{B} + \theta_{out,t} \right) \quad (19)$$

where  $R = B / (C_a V \rho_a)$ .

## 2) The Modeling of the HVAC system with CWS

In the air conditioning industry, CWS systems are one type of cool thermal storage technology that can be used to shift the electrical load from the peak periods to off-peak periods.

A general HVAC system with CWS is composed of chiller compressors, a chilled water storage tank, chilled water pumps for charging/discharging the tank and auxiliary pipelines. Both chillers and discharging of the tank can provide cold for industrial plants. The total cooling power provided by the HVAC system with CWS at time slot  $t$  is formulated as

$$Q_{c,t} = Q_{p,t} - Q_{x,t} + Q_{f,t} \quad (20)$$

where  $Q_{p,t}$ ,  $Q_{x,t}$  and  $Q_{f,t}$  are the cold provided by the chillers, the cold charged and discharged by the chilled water pump within each time slot respectively.

Accordingly, the electric power  $P_{c,t}$  of the HVAC system with CWS at time slot  $t$  can be formulated as

$$P_{c,t} = \frac{Q_{p,t}}{\mu_p} + \mu_x Q_{x,t} + \mu_f Q_{f,t} \quad (21)$$

where  $\mu_p$  is the coefficient of performance (COP) of the chillers;  $\mu_x$  is the conversion coefficient between the cold charged and the corresponding electric power consumption;  $\mu_f$  is the similar conversion coefficient for discharging.

Due to the limit of pipeline circuit, CWS cannot charge and discharge cold simultaneously. The charging state variable  $z_{x,t}$  and discharging state variable  $z_{f,t}$  at time slot  $t$  must satisfy the following constraint:

$$0 \leq z_{x,t} + z_{f,t} \leq 1 \quad (22)$$

where  $z_{x,t}$  and  $z_{f,t}$  are both binary variables. For  $z_{x,t}$ , 1 means charging and 0 means not charging, while for  $z_{f,t}$ , 1 means discharging and 0 means not discharging.

To guarantee the normal operation of the HVAC system with CWS, the values of  $Q_{p,t}$ ,  $Q_{x,t}$  and  $Q_{f,t}$  need to be within certain ranges:

$$0 \leq Q_{p,t} \leq Q_p^{\max} \quad (23)$$

$$0 \leq Q_{x,t} \leq z_{x,t} Q_x^{\max} \quad (24)$$

$$0 \leq Q_{f,t} \leq z_{f,t} Q_f^{\max} \quad (25)$$

where  $Q_p^{\max}$ ,  $Q_x^{\max}$  and  $Q_f^{\max}$  are the upper limit of chilled cold, charged cold and discharged cold within each time slot respectively.

For storage balance of the chilled water storage tank at time slot  $t$ , the following constraint needs to be satisfied:

$$C_{c,t+1} = (1 - \varepsilon) \left( C_{c,t} + (\eta_x Q_{x,t} - \frac{Q_{f,t}}{\eta_f}) \Delta t \right) \quad (26)$$

where  $C_{c,t}$  is cold storage in the storage tank;  $\eta_x$  and  $\eta_f$  are the efficiency of cold charging and cold discharging;  $\varepsilon$  is the self-consumption coefficient.

The storage constraint in the storage tank at time slot  $t$  is expressed as

$$0 \leq C_{c,t} \leq C_c^{\max} \quad (27)$$

where  $C_c^{\max}$  is the capacity of the chilled water storage tank.

## D. EVs Model with V2G Technology

The EVs with V2G technology can provide power to the industrial facility or the main grid while parked at industrial plants. Reasonable charging/discharging of EVs may reduce the costs of the industrial facility.

For an industry with shift  $N$ , the number of workers  $W_n$  is assumed to be constant in each shift  $n$ . The number of EVs at each time slot can be formulated as

$$E_n = \eta_{ev} W_n \quad (28)$$

where  $\eta_{ev}$  is the proportion of workers who use EVs as means of transportation.

In a specific shift  $n$ , i.e., for  $t \in \left[ (n-1) \frac{T}{N} + 1, n \frac{T}{N} \right]$  ( $T$  is the length of the shift), each EV  $e$  has two binary variables  $y_{e,ch,t}$  and  $y_{e,dis,t}$  to represent its charge and discharge state. In each time slot, EV cannot charge and discharge simultaneously, as constrained by

$$0 \leq y_{e,ch,t} + y_{e,dis,t} \leq 1 \quad (29)$$

which guarantees that  $y_{e,ch,t}$  and  $y_{e,dis,t}$  cannot equal to 1 at the same time slot.

The charge and discharge power constraints are expressed as

$$0 \leq P_{e,ch,t} \leq y_{e,ch,t} P_{ch}^{\max} \quad (30)$$

$$0 \leq P_{e,dis,t} \leq y_{e,dis,t} P_{dis}^{\max} \quad (31)$$

where  $P_{e,ch,t}$  and  $P_{e,dis,t}$  are the charge and discharge power of an EV;  $P_{ch}^{\max}$  and  $P_{dis}^{\max}$  are the upper power limit for charging and discharging.

The state of charge (SOC) evolves as follows:

$$SOC_{e,t+1} = SOC_{e,t} + \frac{P_{e,ch,t} \eta_{ch} \Delta t}{C_b} - \frac{P_{e,dis,t} \Delta t}{C_b \eta_{dis}} \quad (32)$$

where  $\eta_{ch}$  and  $\eta_{dis}$  are the charge and discharge efficiency of an EV;  $C_b$  is the battery capacity of an EV.

The state of charge (SOC) should be within certain range:

$$SOC_e^{down} \leq SOC_{e,t} \leq SOC_e^{up} \quad (33)$$

where  $SOC_e^{down}$  and  $SOC_e^{up}$  are the lower and upper limits of SOC.

For the sake of battery life, the times of charging/discharging state transition should not exceed certain value:

$$y_t \geq y_{e,dis,t} - y_{e,dis,t+1} \quad (34)$$

$$y_t \geq y_{e,dis,t+1} - y_{e,dis,t} \quad (35)$$

$$\sum_{t=1+(n-1)T_n}^{nT_n} y_t \leq y_{dis} \quad (36)$$

where  $y_t$  is an indicator for recording charging/discharging state transition;  $y_{dis}$  is the limit of the transition times.

The SOC constraint when EV leaves is expressed as

$$SOC_e^{set} \leq SOC_e \left( n \frac{T}{N} \right) \leq 1 \quad (37)$$

where  $SOC_e^{set}$  is the minimum SOC preset for the time EV leaves the industrial plant;  $n \frac{T}{N}$  represents the end time slot of the shift  $n$ , at which the workers leave.

### E. Energy Cost Minimization for the Industrial Facility

#### 1) Objective Function

The objective of IIEM is to minimize the total electricity costs to the industrial facility given time-of-use electricity prices. The costs equal to the cost of purchasing electricity minus the income from selling electricity to the power utility, formulated as

$$\min \left( \sum_{t=1}^T c_{p,t} P_{p,t} \Delta t - \sum_{t=1}^T c_{s,t} P_{s,t} \Delta t \right) \quad (38)$$

where  $c_{p,t}$  and  $c_{s,t}$  are the unit price of purchasing and selling electricity at time slot  $t$ ;  $P_{p,t}$  and  $P_{s,t}$  are the amount of electricity purchased from the utility and sold to the utility at time slot  $t$ , both of which are nonnegative, with 0 indicating no purchasing and selling.

#### 2) Electricity balance constraints

The electricity balance constraint is expressed as

$$P_{p,t} + P_{g,t} + \sum_{e=1}^{E_{n,t}} P_{e,dis,t} = P_{s,t} + \sum_{i=1}^I P_{i,t} + P_{c,t} + \sum_{e=1}^{E_{n,t}} P_{e,ch,t} + P_{fix,t} \quad (39)$$

where  $P_{g,t}$  and  $P_{fix,t}$  are the active power of PV generation and fixed demand of the industrial facility.  $I$  represents the amount of industrial tasks.

A pair of binary variables,  $v_{p,t}$  and  $v_{s,t}$ , are defined to indicate whether the industrial facility purchase/sell electricity from/to the main power grid.  $v_{p,t} = 1$  indicates that the industrial customer purchases electricity while  $v_{s,t} = 1$  indicates that the electricity is sold to the main grid.  $v_{p,t}$  and  $v_{s,t}$  cannot be 1 at the same time:

$$0 \leq v_{p,t} + v_{s,t} \leq 1 \quad (40)$$

In addition, the amount of electricity purchased from the utility and sold to the utility should be under certain limit:

$$0 \leq P_{p,t} \leq v_{p,t} P_p^{\max} \quad (41)$$

$$0 \leq P_{s,t} \leq v_{s,t} P_s^{\max} \quad (42)$$

where  $P_p^{\max}$  and  $P_s^{\max}$  are the upper limit of electricity purchased from and sold to the utility.

So far, the IIEM model has been formulated as a MILP problem, which can be solved by existing tools such as CPLEX and YALMIP [22]. The solution solved from the optimization problem is the optimal operation plan for the industrial facility. In this paper we assume that day-ahead scheduling is conducted.

## III. CASE STUDY

### A. Scenario Settings

A three-shift tire manufacturing facility is used as a case study, and day-ahead time-of-use pricing (TOUP) is assumed as the pricing scheme considered. The scheduling horizon is one day (24h) with each time slot equal to 1h. It is assumed that the power generated by PV systems has a unified feed-in tariff, being 0.88 yuan/kWh. The PV power generation and ambient temperature are illustrated in Fig. 2. The required temperature in the plant and the minimum amount of the final product are set to 20°C and 3300 respectively.

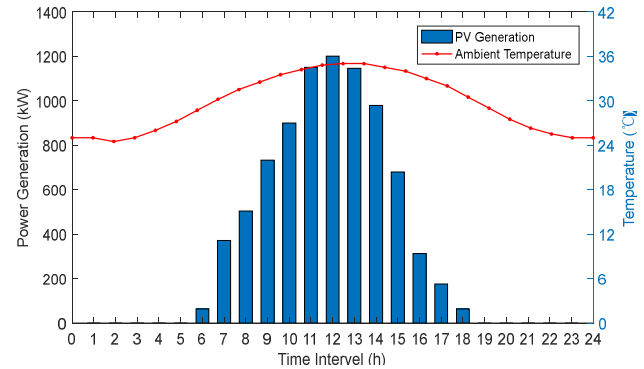


Fig. 2. Data of PV generation and ambient temperature.

Fig. 3 shows the simplified STN representation of the tire industry, where the roundness represents state nodes and rectangle represents task nodes. The parameters related to the task nodes are listed in Table I and Table II. It is assumed that in the end of scheduling horizon  $T$ , the facility does not undertake industrial production tasks.

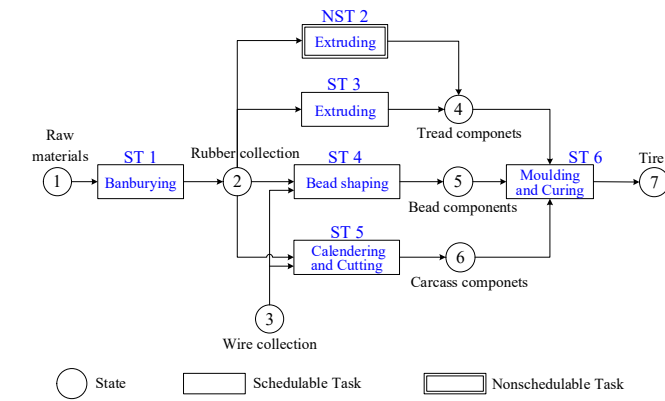


Fig. 3. STN representation of the tire facility.

TABLE I  
PARAMETERS RELATED TO THE TASK NODES – PART I

$i$	$k$	$P_i$ (kW)	$W_i$	$Q_i$ (kW)
1	1	450	10	225
	2	600	20	300
	3	750	30	375
2	1	200	30	100
3	1	100	20	50
	2	200	30	100
4	1	60	20	30
	2	100	30	50
5	1	240	20	120
	2	300	30	150
	3	450	40	225
6	1	450	30	225
	2	600	40	300
	3	750	50	375

TABLE II  
PARAMETERS RELATED TO THE TASK NODES – PART II

$i$	$k$	$a_{i,j,k}$ (ton/h)			$b_{i,j,k}$ (ton/h)
1		From State Node 1	-	-	To State Node 2
	1	1.7	-	-	1.5
	2	2.2	-	-	2
	3	2.8	-	-	2.5
2		From State Node 2	-	-	To State Node 4
	1	1.1	-	-	1
3		From State Node 2	-	-	To State Node 4
	1	0.55	-	-	0.5
	2	1.1	-	-	1
4		From State Node 2	From State Node 3	-	To State Node 5
	1	0.27	0.03	-	0.3
	2	0.45	0.05	-	0.5
5		From State Node 2	From State Node 3	-	To State Node 6
	1	0.72	0.08	-	0.8
	2	0.9	0.1	-	1

	3	1.35	0.15	-	1.5
6		From State Node 4	From State Node 5	From State Node 6	To State Node 7 (/h)
	1	0.6	0.3	0.6	150
	2	0.8	0.4	0.8	200
	3	1	0.5	1	250

Table III and Table IV show the related parameters of CWS and EVs. The parameters for each shift are given in Table V.

TABLE III  
PARAMETERS OF THE HVAC SYSTEM WITH CWS

$Q_p^{\max}$ (kW)	$Q_x^{\max}$ (kW)	$Q_f^{\max}$ (kW)	$C_c^{\max}$ (MWh)	$B$ (kW/°C)	$R$ (kJ/°C)
2100	1800	1800	10	15.3	6055.125
$\eta_x$	$\eta_f$	$\varepsilon$	$\mu_p$	$\mu_x$	$\mu_f$
0.95	0.92	0.035	5	0.008	0.007

TABLE IV  
PARAMETERS OF ELECTRIC VEHICLES

$P_{ch}^{\max}$ (kW)	$P_{dis}^{\max}$ (kW)	$\eta_{ch}$	$\eta_{dis}$	$C_b$ (kWh)	$SOC_e^{down}$	$SOC_e^{up}$	$SOC_e^{set}$
3.3	3.3	0.95	0.95	24	0.2	1	0.9

TABLE V  
PARAMETERS OF THE THREE SHIFTS

Shift	$W_n$	$W_n^{fix}$	$E_n$ ( $\eta_{ev}=0.8$ )	$q_w$ (kW)
1	50	10	40	0.08
2	200	20	160	0.12
3	150	10	120	0.1

Three scenarios were considered in the case study:

- (i) Scene 1: Reference scenario without PV generation and DR.
- (ii) Scene 2: With no PV generation but with DR implemented.
- (iii) Scene 3: With PV generation and DR implemented.

### B. Simulation Results

#### 1) Total Power Consumption, Energy Cost and Energy Use

Fig. 4 shows the comparison of electricity demand in the three scenarios, where the positive and negative values represents the electricity purchasing and selling respectively. The corresponding electricity costs and electricity uses are given in Table VI and Table VII.

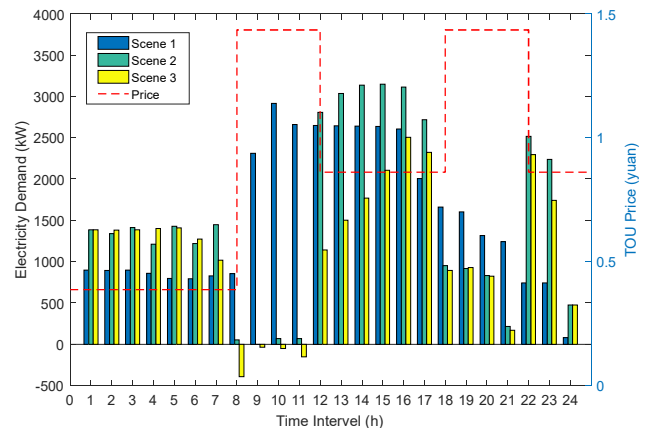


Fig. 4. Electricity purchased/sold in the three scenarios.

Fig. 4 shows that scene 2 and scene 3 are able to shift the electricity demand during peak time intervals (from 08:00 to 11:00 and from 18:00 to 21:00) to other times, as a result of the optimal scheduling of IEM. Due to the production constraints such as restrictions on the number of workers, in both scene 2 and scene 3, the electricity demand of peak periods are dispersed to both low-price and mid-price periods rather than be just shifted to the time intervals with the lowest price (from 0:00 to 08:00). In scene 3, the tire manufacturing facility is able to benefit from selling excess electricity to the power utility on account of the PV generation from 08:00 to 11:00.

TABLE VI  
ELECTRICITY COSTS IN THE THREE SCENARIOS

Scenes	Process (yuan)	HVAC system with CWS (yuan)	EVs (yuan)	Purchase (yuan)	Sell (yuan)	Cost (yuan)
1	26967	4468	2874	35335	-	35335
2	23015	3026.2	3636	28079	-	28079
3	23482	3013	2299	21274	557	20717

Notes: The cost of fixed demand is 1026 yuan.

Table VI counts the total electricity costs in the three scenarios. Compared to scene 1, the total electricity cost of scene 2 and scene 3 have declined significantly because of the DR implemented. Compared with scene 2, the electricity cost of scene 3 is further reduced by about 26% because of the installation of PV generation.

TABLE VII  
ELECTRICITY USES AND IMPORT/EXPORT IN THE THREE SCENARIOS

Scenes		Scene 1	Scene 2	Scene 3
Energy Use	Fixed demand (kWh)	1025	1025	1025
	Industrial process (kWh)	27280	26830	26830
	HVAC with CWS (kWh)	4436	5157	5139
EV charging (kWh)		2528	4555	3003
EV discharging (kWh)		0	1830	429
PV generation (kWh)		-	-	8274
Total energy import (kWh)		35269	35737	27928
Total energy export (kWh)		0	0	634

In Table VII, the energy use of components, and energy import and export of the facility are presented. First of all, it is seen that the total electricity import of scene 2 (conducting demand response) was slightly higher than that of scene 1 (not conducting demand response), due to the increased energy consumption of HVAC system with CWS and EV charging. In scene 2, the cooling energy was charged in CWS during low-price periods and discharged during high-price periods, which reduced the electricity bill but increased the electricity consumption because of the energy loss in the charging and discharging processes (as detailed in Equation (21) and (26)). Similarly, in scene 2, EV charged more during low-price periods for discharging during high-price periods, which

resulted in more electricity import and energy loss as well. Comparing scene 2 and scene 3 (both with demand response but scene 3 having PV generation), it is found that the total electricity import throughout the day reduced significantly because of the existence of local generation, and there was even some electricity exported to the main grid. Also, in scene 3, EV charged and discharged less compared to that of scene 2, because a lot of loads at high-price periods in the daytime have been supplied by local generation, reducing the need for transporting energy from low-price periods.

2) Power Consumption of Industrial Processes

By the comparison of Fig. 5, we can see that under the guidance of the electricity price signal, the electricity demand of industrial processes in peak periods has been greatly reduced, but this demand has not been totally shifted to the lowest electricity price period. This is because from 00:00 to 07:00, all schedulable tasks are restricted by the number of workers and the production cannot be further increased.

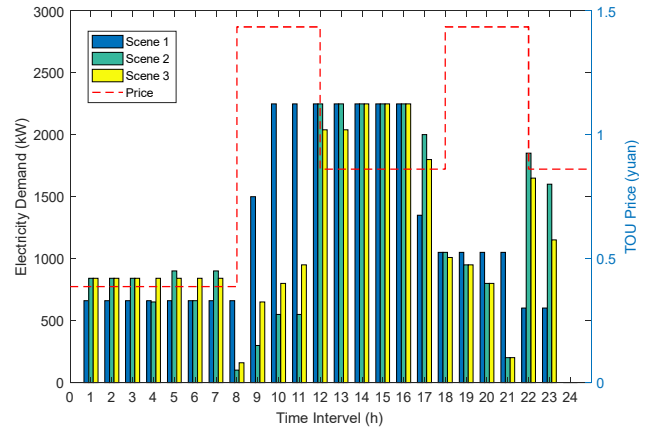


Fig. 5. Electricity demand of industrial processes in the three scenarios.

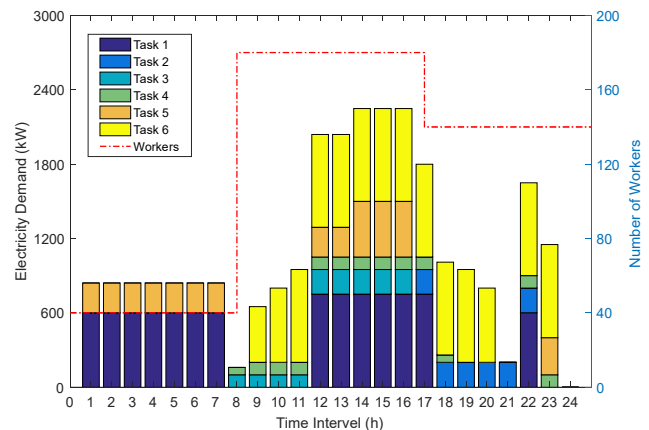


Fig. 6. Industrial processes scheduled in scene 3.

Fig. 6 clearly shows the various production tasks of scene 3. The number of workers from 0:00—07:00 is only 40 and the production of scene 3 is strictly limited to the constraints. It can be seen that the STN-based production model used in this paper reflects the actual industrial production process, and the constraints on production conditions (e.g. the number of workers) limit the flexibility of the production electricity.

Due to the influence of PV power generation, scene 2 and scene 3 have different electricity demand during peak electricity price periods. In the three hours from 08:00 to 11:00, the power consumption in scene 2 is 100 kW, 500 kW and 350 kW while in scene 3 is 160 kW, 650 kW and 800kW respectively. That is, more electricity is consumed during the peak price periods in scene 3 than that in scene 2. This is because when the feed-in tariff is lower than the purchasing price, more electricity demand will be shifted to the periods with excess PV generation (even the periods are with high electricity price) to consume the cheap excess PV power generation.

### 3) Power Consumption of the HVAC system with CWS

In scene 2 and scene 3, the IIEM responds to the electricity price signal by adjusting the power of the HVAC system with CWS while still satisfying the temperature requirements in the production environment. The electricity demand of the HVAC system with CWS in the three scenarios are shown in Fig. 7, and the demand profiles in scene 3 are shown in Fig. 8.

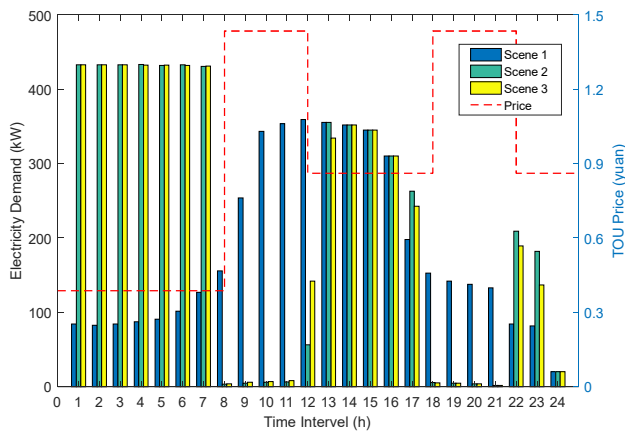


Fig. 7. Electricity demand of TCLs in the three scenarios.

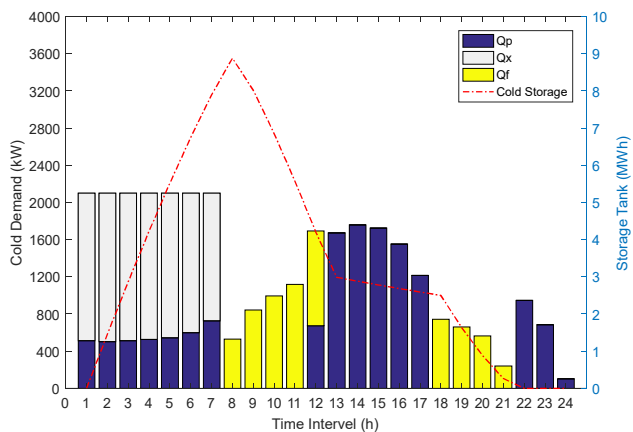


Fig. 8. The demand profiles of the HVAC system with CWS in scene 3.

Combined with Fig. 7 and Fig. 8, we can see that in the scenes with DR, the electricity demand of the HVAC system with CWS is shifted from two peak periods (from 08:00 to 11:00 and 18:00 to 21:00) to the lowest price periods of the night time (from 0:00 to 07:00). The chillers refrigerate at night to use low-cost electricity and store cold in the storage tank, and

the pump discharges in peak periods to maintain the desired temperature environment. Due to the capacity limitation of the storage tank and the minimization of the cost, the cold in the mid-price periods (from 13:00 to 17:00 and 22:00 to 24:00) is provided by the chillers instead of the storage tank.

### 4) Power Consumption of EVs

In the scene 1, EVs does not charge according to the price signals. Each EV is charged at maximum power in the beginning of each shift until up to its desired SOC. In contrast, IIEM with DR are applied in scene 2 and scene 3. From Fig. 9 (where bars represent the charging profiles and lines represent discharging profiles), we can see that in scene 2, the EVs prefer to discharge during peak periods in shift 2 (from 08:00 to 11:00) and shift 3 (from 18:00 to 21:00), and charge more in other off-peak periods to minimize total electric cost. Due to the PV generation in scene 3, the EVs choose to charge during off-peak periods from 12:00 to 16:00 and discharge during peak periods from 18:00 to 21:00.

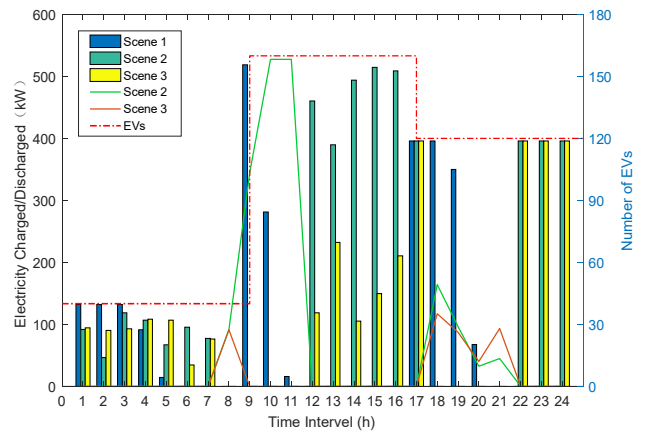


Fig. 9. Charging/discharging profiles in the three scenarios.

### 5) The Effect of Length of Time Slots on Optimization Results

Generally, the mathematical models of intelligent industrial energy management (IIEM) formulated in this paper are applicable for any length of time steps. In the previous case studies, the length of time slots were taken as 1 hour. This section examines the impact of the length of time slots on the optimization results of the industrial facility. Three different length of time slots were studied and the results are presented in Table VIII.

TABLE VIII  
OPTIMIZATION RESULTS GIVEN DIFFERENT LENGTH OF TIME SLOTS

Scene	Total cost of the whole facility (yuan)		
	$\Delta t = 60 \text{ min}$	$\Delta t = 30 \text{ min}$	$\Delta t = 15 \text{ min}$
2	28079	27879	27283
3	20717	20655	20583

In Table VIII, it is seen that the electricity cost of the whole facility keeps decreasing with the decrease of the length of time slots. This is because with smaller time slots, more delicate scheduling can be conducted, which will lead to better results. However, it is also observed that the improvement due to the decrease of length of time slots is quite limited. For Scene 2 and

3, comparing the scenarios with 15-minute and 60-minute time slots, the savings of the whole facility are only 2.8% and 0.6% respectively.

It is worth noting that although theoretically smaller time slots always result in non-worse optimization results, generally we do not select very small time slots due to the following reasons: 1) the improvement becomes trivial with the decreasing length of time slots; 2) the proposed IEM is a mixed integer linear programming problem, for which the computational burden will increase exponentially with the decreasing length of time slots (i.e. with the increasing number of decision variables); 3) in practice the PV forecast has inevitable uncertainties, so minor improvement in day-ahead scheduling does not necessarily mean lower cost in real operation. Therefore, in practice, sensitivity studies, like the one did in this section, can be done, and a roughly reasonable length of time slot can be chosen as the ones for which the decreasing length of time slots cannot bring significant cost savings. The computational burden and the level of uncertainties in PV generation can also be considered. For example, for this case, actually the time slots ranging from 15 minutes to 60 minutes are all somehow acceptable, because the improvement brought by decreasing the length of time slots has already been quite small.

6) *Sensitivity Study for estimation error*

In the previous analysis, the results were derived based on the assumption that accurate information was available for the parameters including electricity prices, ambient temperature and PV generation. In practice, time-of-use prices are usually known in advance as in China and many other countries of the world, but uncertainties in the forecast of ambient temperature and PV generation are inevitable. These uncertainties may undermine the performance of the schedules obtained by the proposed IEM.

Therefore, an error sensitivity study was conducted to examine the impact of the uncertainties and the robustness of the proposed IEM. As usually assumed [23], [24], the forecast errors of ambient temperature and PV generation were assumed to follow a normal distribution, with the mean being 0 and the standard deviation being 10%. Then the parameter values used in scene 3 were assumed as the forecast values, and the actual values were assumed to be the forecast value plus the errors sampled from the normal distribution. A number of scenarios were generated and calculated, and the results under these scenarios are summarized in Table IX.

TABLE IX  
SENSITIVITY STUDY OF TOTAL COST OF THE FACILITY

Parameters considered with uncertainties	Expected cost (yuan)	Actual cost	
		Mean (yuan)	Standard Deviation (yuan)
PV generation	20717	20702	231.5
Ambient temperature $\theta_{out}$	20717	20723	35.6

In Table IX, the expected cost means the cost if the forecast is accurate. It is seen that for both PV generation and ambient

temperature, even with uncertainties considered, the mean actual costs were still very close to the expected costs, showing the good robustness of the proposed IEM. It is also seen that the uncertainty of PV generation will cause higher variance in the results, with a standard deviation being 231.5 yuan. In contrast, the impact of the uncertainty of ambient temperature was less significant, with the standard deviation being only 35.6 yuan.

IV. CONCLUSION

A new optimization-based IEM framework was proposed for industrial facilities with PV generation and DR potential. The framework includes multiple modules including industrial processes modeled with the STN method, the HVAC system with CWS as TCLs, PV panels as renewable distributed generation and EVs with V2G capability. The modules are closely coupled with each other by the factors such as the number of workers, and contain great flexibility to be utilized. The IEM with DR was formulated as an MILP problem, and the obtained solution yields optimal operation plans for industrial facilities.

Case studies were carried out in a general tire manufacturing facility with three scenarios designed. The electricity demands and costs of different parts of the facility were presented and compared. Simulation results verified that the proposed IEM with DR is able to effectively utilize the flexibility contained in all parts of the facility and reduce the electricity costs as well as the peak demand of the facility, while satisfying all the operating constraints.

The proposed IEM has good generalizability and can be applied to many other industrial facilities besides the tire manufacturing facilities demonstrated in this paper. The reason is mainly threefold: 1) the STN model used in the formulation has good generalizability, which has already been applied to chemical plants [19], pharmaceutical industries [25], steel manufacturing facilities [7], oxygen generation facilities [11], car seat manufacturing plants [18], etc.; 2) the models of EVs, PV generation and TCLs have little difference for different industrial facilities, so the ones used in the proposed IEM are naturally applicable; 3) the proposed IEM optimizes the electricity bill in a time-of-use pricing scheme, which has been widely adopted in many countries and regions across the world. Therefore, to summarize, the proposed IEM has the potential to be used for optimizing the operation of many industrial facilities in many countries in the future, resulting in positive practical significance.

In this paper, the proposed IEM does not include energy storage explicitly. However, the proposed IEM can be applied to industrial facilities with energy storage easily, because to schedule EVs is in nature to schedule the charging and discharging of the batteries on the EVs. To a great extent, energy storage can be seen as EVs that will always stay in the industrial facility, without any travel need. Therefore, the proposed IEM does not lose any generality in this sense, and can be applied to optimize the operation of industrial facilities with energy storage.

Energy storage, as a highly flexible resource, may increase

the revenue of industrial facilities by arbitraging in time-of-use or other flexible pricing schemes. Furthermore, energy storage can increase the on-site consumption of local generation (e.g. PV generation considered in this paper) to further reduce the electricity bill. However, energy storage is still costly in many cases, despite its fast decreasing cost. Therefore, it is necessary to study what types and how much capacity of energy storage should be installed for industrial facilities to ensure the cost-effectiveness. This paper focuses on the operation scheduling rather than sizing of equipment. The optimal sizing of energy storage in industrial facilities, or other new equipment like PV generation, is a direction for future research.

REFERENCES

[1] J. S. Vardakas, N. Zorba and C. V. Verikoukis, "A survey on demand response programs in smart grids: Pricing methods and optimization algorithms," *IEEE Communications Surveys & Tutorials*, vol. 17, no. 1, pp. 152-178, Mar. 2015.

[2] M. Beaudin and H. Zareipour, "Home energy management systems: A review of modelling and complexity," *Renewable & Sustainable Energy Reviews*, vol. 45, pp. 318-335, Feb. 2015.

[3] M. Macarulla, M. Casals, and N. Forcada, "Implementation of predictive control in a commercial building energy management system using neural networks," *Energy & Buildings*, vol. 151, pp. 511-519, Jun. 2017.

[4] S. L. Arun and M. P. Selvan, "Intelligent Residential Energy Management System for Dynamic Demand Response in Smart Buildings," *IEEE Systems Journal*, vol. 12, no. 2, pp. 1329-1340, Jan. 2017.

[5] T. Samad and S. Kiliccote, "Smart grid technologies and applications for the industrial sector," *Computers & Chemical Engineering*, vol. 47, pp. 76-84, Jul. 2012.

[6] National Energy Administration, National power industry statistics in 2017. Beijing, China, Jan. 2018. [Online]. Available: [http://www.nea.gov.cn/2018-01/22/c\\_136914154.htm](http://www.nea.gov.cn/2018-01/22/c_136914154.htm).

[7] Y. M. Ding and S. H. Hong, "A model of demand response energy management system in industrial facilities," in *Proc. IEEE Int. Conf. Smart Grid Commun.*, Vancouver, BC, Canada, Dec. 2013, pp. 241-246.

[8] A. Gholian, H. Mohsenian-Rad, Y. Hua, and J. Qin, "Optimal industrial load control in smart grid: A case study for oil refineries," in *Proc. IEEE PES Gen. Meeting*, Vancouver, BC, Canada, Jul. 2013, pp. 1-5.

[9] A. Gholian, H. Mohsenian-Rad and Y. Hua, "Optimal industrial load control in smart grid," *IEEE Trans. Smart Grid*, vol. 7, no. 5, pp. 2305-2316, Sep. 2016.

[10] S. Bahrami, F. Khazaeli, and M. Parniani, "Industrial load scheduling in smart power grids," in *Proc. IEEE CIREED*, Stockholm, Sweden, Dec. 2013, pp. 1-4.

[11] Y. M. Ding and S. H. Hong and X. L. Li, "A demand response energy management scheme for industrial facilities in smart grid," *IEEE Trans. Ind. Informat.* vol. 10, no. 4, pp. 2257-2269, Nov. 2014.

[12] C. C. Yan, X. Xue, S.W.Wang and B. Cui, "A novel air-conditioning system for proactive power demand response to smart grid," *Energy Conversion & Management*, vol. 102, pp.239-246, Oct. 2015.

[13] W. M. Lin, C. S. Tu and M. T. Tsail, "Optimal Energy Reduction Schedules for Ice Storage Air-Conditioning Systems," *Energies*, vol. 8, no. 9, pp.10504-10521, Sep. 2015.

[14] J. F. O. Giron, *Optimal Load Management Application for Industrial Customers*. Waterloo, Canada, 2015, pp. 677-693.

[15] E V Committee, "Annual report on technical and industrial development of electric vehicle power supply and drive in China," *Advanced Technology of Electrical Engineering & Energy*, vol. 34, no. 7, Jul. 2015.

[16] J. F. Franco, M. J. Rider and R. Romero, "An MILP model for the plug-in electric vehicle charging coordination problem in electrical distribution systems," in *Proc. IEEE PES Gen. Meeting*, Washington, DC, USA, Jul. 2014, pp. 1-5.

[17] C. F. Sabillon A, J. F. Franco, M.J. Rider and R. Romero, "A MILP model for optimal charging coordination of storage devices and electric vehicles

considering V2G technology" in *Proc. IEEE Int. Conf. Environment & Electrical Engineering.*, Rome, Italy, Jul. 2015, pp. 60-65.

[18] J. Y. Shi, F. C. Wen, Cui and L. Sun, "Intelligent energy management of industrial loads considering participation in demand response program," *Automation of Electric Power Systems*, vol. 41, no. 14, pp. 45-53, Jul. 2017.

[19] E. Kondili, C. C. Pantelidest, and R.W. H. Sargent, "A general algorithm for short-term scheduling of batch operations—I. MILP formulation," *Comput. Chem. Eng.*, vol. 17, no. 2, pp. 211-227, Feb. 1993.

[20] Q. S. Xu, C. X. Yang and G. Q. Yan, "Strategy of day-ahead power peak load shedding considering thermal equilibrium inertia of large-scale air conditioning loads," *Power System Technology*, vol. 40, no. 1, pp. 156-163, Jan. 2016.

[21] *Practical Design Manual for Heating and Air Conditioning*, China Architecture & Building Press., Beijing, China, 2007.

[22] R. Kia, P. Shahnazari-Shahrezaei and S. Zabihi, "Solving a multi-objective mathematical model for a Multi-Skilled Project Scheduling Problem by CPLEX solver," in *Proc. IEEE Int. Conf. on Industrial Engineering & Engineering Management.*, Bali, Indonesia, Dec. 2016, pp. 1220-1224.

[23] Z. Zakaria, O. Masato and S. Tomonob, "Optimal Voltage Control Using Inverters Interfaced With PV Systems Considering Forecast Error in a Distribution System," *IEEE Trans. Sustainable Energy*, vol. 5, no. 2, pp. 682-690, Apr. 2014.

[24] J. D. Wang, Y. Q. Li and Y. Zhou, "Interval number optimization for household load scheduling with uncertainty," *Energy & Buildings*, vol. 130, pp. 613-624, Aug. 2016.

[25] S. Kabra, M. A. Shaik and A. S. Rathore, "Multi-period scheduling of a multi-stage multi-product bio-pharmaceutical process," *Computers & Chemical Engineering*, vol. 57, no. 20, pp. 95-103, Oct. 2013.



**Jidong Wang** (M'16) received his B.S. and M.S. degrees from Shandong University of Technology and Shandong University, Shandong, China, in 1999 and 2002 respectively, and his Ph.D. degree in electrical engineering from Tianjin University, Tianjin, China, in 2005. He worked as a post-doctoral from 2005 to 2007 and became an Associate Professor from 2007 to 2017 in Tianjin University. Currently, he is a Professor with the School of Electrical and Information Engineering, Tianjin University. His research interests include power quality, distributed generation, microgrid and smart power consumption.



**Yingchen Shi** was born in Jiangxi, China, in 1995. She obtained her B.S. degree in electrical engineering and automation from China Agricultural University, Beijing, China, in 2016. She is currently pursuing the M.S. degree in electrical engineering at Tianjin University, Tianjin, China. Her main research interest is electric vehicle and smart power utilization.



**Yue Zhou** (M'13) received his B.S., M.S. and Ph.D. degrees in electrical engineering from Tianjin University, Tianjin, China, in 2011, 2016 and 2016, respectively. He is currently a post-doctoral research associate at School of Engineering, Cardiff University, Wales, UK. His research interests include demand response, frequency response, smart home energy management, optimization and blockchain technology.